

## A continuous fluorometric assay for the assessment of MazF ribonuclease activity

Nora R. Wang, Paul J. Hergenrother \*

*Department of Chemistry, Roger Adams Laboratory, University of Illinois, Urbana, IL 61801, USA*

Received 4 June 2007

Available online 26 July 2007

### Abstract

Plasmids maintain themselves in their bacterial host through several different mechanisms, one of which involves the synthesis of plasmid-encoded toxin and antitoxin proteins. When the plasmid is present, the antitoxin binds to and neutralizes the toxin. If a plasmid-free daughter cell arises, however, the labile antitoxin is degraded (and not replenished) and the toxin kills the cell from within. These toxin–antitoxin (TA) systems thereby function as postsegregational killing systems, and the disruption of the TA interaction represents an intriguing antibacterial strategy. It was recently discovered that the genes for one particular TA system, MazEF, are ubiquitous on plasmids isolated from clinical vancomycin-resistant enterococci (VRE) strains. Thus, it appears that small molecule disruptors of the MazEF interaction have potential as antibacterial agents. The MazF toxin protein is known to be a ribonuclease. Unfortunately, traditional methods for the assessment of MazF activity rely on the use of radiolabeled substrates followed by analysis with polyacrylamide gel electrophoresis. This article describes a simple and convenient continuous assay for the assessment of MazF activity. The assay uses an oligonucleotide with a fluorophore on the 5' end and a quencher on the 3' end, and processing of this substrate by MazF results in a large increase in the fluorescence signal. Through this assay, we have for the first time determined  $K_M$  and  $V_{max}$  values for this enzyme and have also found that MazF is not inhibited by standard ribonuclease inhibitors. This assay will be useful to those interested in the biochemistry of the MazF family of toxins and the disruption of MazE/MazF.

© 2007 Elsevier Inc. All rights reserved.

**Keywords:** Toxin–antitoxin systems; High-throughput screening; Antibacterials; Antibiotics; Protein–protein disruption

Once regarded as a microbiological curiosity, it is now apparent that toxin–antitoxin (TA)<sup>1</sup> systems play important roles in bacterial stress response and resistance to antibiotics [1–3]. Most proteic TA systems are characterized by two small proteins (8–15 kDa), a stable toxin and a labile antitoxin, and genes encoding these proteins have been

identified on a wide range of bacterial chromosomes and plasmids [4,5]. If both proteins are actively being produced by the bacterial cell, the antitoxin binds the toxin and inhibits its toxic activity. However, if the cellular levels of the antitoxin drop, the toxic protein will be unleashed to halt growth and/or kill the cell.

When encoded by plasmids, TA systems serve as a postsegregational killing system [6] that allows the plasmid to maintain itself in the bacterial population in the absence of selective pressure. If a plasmid-free daughter cell arises during cell division, the labile antitoxin is quickly degraded (and is not replenished due to the absence of plasmid), freeing the toxin to kill the cell [1]. Such TA systems sometimes are referred to as “plasmid addiction” modules [7,8]. The precise role of TA systems encoded by bacterial chromosomes is less clear, but there is evidence that they may serve

\* Corresponding author.

*E-mail address:* [hergenro@uiuc.edu](mailto:hergenro@uiuc.edu) (P.J. Hergenrother).

<sup>1</sup> *Abbreviations used:* TA, toxin–antitoxin; VRE, vancomycin-resistant enterococci; MALDI, matrix-assisted laser desorption/ionization; 6-FAM, 6-carboxyfluorescein; BHQ1, Black Hole Quencher 1; BSA, bovine serum albumin; IPTG, isopropyl  $\beta$ -D-1-thiogalactopyranoside; Ni-NTA, nickel-nitrilotriacetate; HPLC, high-performance liquid chromatography; TEAA, triethylammonium acetate; RFU, relative fluorescence units; DTT, dithiothreitol; pAp, adenosine 3',5'-diphosphate; RI, ribonuclease inhibitor protein.

as stress response elements given that toxin-induced cell death is observed under conditions that include high temperature, DNA damage, oxidative stress [9], thymine starvation [10], and antibiotic treatment [11]. In addition, the transcription of genes from chromosomally encoded TA loci is upregulated during amino acid starvation [12,13].

Given that a large percentage of genes that mediate resistance to antibiotics are found on extrachromosomal DNA such as plasmids [14,15], coupled with the ability of TA systems to stabilize plasmids, it has been speculated that pharmacological disruption of the TA protein–protein interaction could unleash the toxin and be a novel antibacterial strategy [2,5,16,17]. It was not until recently, however, that it was discovered that TA systems are indeed ubiquitous on plasmids that reside in a common bacterial pathogen that is refractory to most antibiotics, namely, vancomycin-resistant enterococci (VRE) [5]. In that study, the genes encoding the *mazEF*, *relBE*, and *axe-txe* TA systems were found to be quite prevalent on plasmids isolated from clinical VRE isolates. In particular, the *mazEF* genes were found on plasmids in 100% (75/75) of the VRE isolates [5].

*MazEF* originally was discovered on the *Escherichia coli* chromosome [18,19] and has since been characterized extensively. Much is known about the TA protein complex given that the crystal structure of the toxin, MazF, in complex with the antitoxin, MazE, has been solved [20]. The MazEF complex has a heterohexamer structure, with two MazF homodimers flanking a single MazE homodimer. The C terminus of each MazE monomer wraps around the interface of each MazF homodimer to neutralize MazF toxicity. It was only recently, however, that the toxic effect of MazF was tied conclusively to its ribonuclease activity [21,22]. MazF is known to have a specificity for ACA sequences in single-stranded RNA, typically cleaving after the first A, although cleavage before the first A has also been observed [23,24].

No detailed analysis of the kinetics of the MazF-mediated cleavage of RNA is available, and such studies are hampered by the lack of a convenient method for the assessment of MazF activity. Until now, MazF activity has been monitored with radiolabeled oligonucleotides/gel electrophoresis or matrix-assisted laser desorption/ionization (MALDI) mass spectrometry [23–25]. Although these techniques have proved to be instrumental in the characterization of MazF activity, such discontinuous methods make the evaluation of multiple substrate types and concentrations prohibitive. This article describes a continuous fluorometric substrate for MazF that enables real-time quantitation of MazF enzymatic activity and full kinetic analysis of this enzyme. We show that this new assay is also suitable for the quantitative evaluation of MazF inhibitors and could be used to screen for disruptors of the MazEF complex in a high-throughput manner.

## Materials and methods

### Materials

Primers, unlabeled oligonucleotides, oligonucleotides of the sequence 5'-AAGTCrGACATCAG-3' labeled with 6-carboxyfluorescein (6-FAM) on the 5' end and with Black Hole Quencher 1 (BHQ1) on the 3' end, and the corresponding oligonucleotide cleavage fragments, 6-FAM-labeled 5'-AAGTCG-3' and BHQ1-labeled 5'-ACATCAG-3', were purchased from Integrated DNA Technologies (Coralville, IA, USA). Black, tissue culture-treated 384-well plates were purchased from Matrix Technologies (Hudson, NH, USA). Protein purification buffers were modified from those described for protein purification under native conditions by Qiagen (Valencia, CA, USA). Binding buffer consisted of 50 mM Tris–Cl (pH 8.0), 300 mM NaCl, and 10 mM imidazole; wash buffer consisted of 50 mM Tris–Cl (pH 8.0), 300 mM NaCl, and 20 mM imidazole; and elution buffer consisted of 50 mM Tris–Cl (pH 8.0), 300 mM NaCl, and 250 mM imidazole.

### Cloning

The *mazEF* gene cassette was amplified by PCR (primers 5'-CACCATGATCCACAGTAGCGTAAAGCGTTGG-3' and 5'-CTACCCAATCAGTACGTTAATTTTGGC-3') using plasmid DNA extracted from a clinical isolate of VRE, namely, SL171RF [5]. Sequence analysis of these *mazEF* loci showed them to be identical to the *mazEF* sequence from the *E. coli* chromosome. Plasmid pKm6EF was then constructed by cloning the amplified *mazEF* gene cassette into the pET200 expression vector using the Champion pET Directional TOPO Expression Kit (Invitrogen, Carlsbad, CA, USA). pKm6EF encodes the MazEF protein complex with an N-terminal histidine-6 tag; thus, in this system, the histidine tag is appended to the N terminus of the MazE protein and the MazF protein is not tagged. To create an expression vector that would result in an untagged MazE and a C-terminally tagged MazF, site-directed mutagenesis of pKm6EF was performed in two rounds to install restriction sites on each end of the *mazEF* gene cassette. The first round introduced an *NcoI* restriction site on the 5' end of the gene (primers 5'-GATAAGGATCATCCCTTACCATGGTCCACAGTAGCGRAAAGCG-3' and 5'-CGCTTACGCTACTGTGGACCATG GTGAAGGGATGATCCTTATC-3'), and the second round of mutagenesis introduced an *XhoI* cut site on the 3' end of the *mazEF* insert and removed the stop codon to allow translation of a 3' histidine tag (primers 5'-GGATCGTTGAGCTCGAGCTTCTTCCAATCAGTACGTTAATTTTGG-3' and 5'-CCAAAATTAACGTAAGTATTGGGAAGAAGCTCGAGCTCAACGATCC-3'). The *mazEF* gene was excised from this mutated pKm6EF plasmid with *NcoI* and *XhoI*, and digestion products were run on a 0.6% agarose gel. The *mazEF* gene cassette was purified by gel extraction

and cloned into the pET28a expression vector (Novagen, San Diego, CA, USA) to construct plasmid pKmEF6.

Each site-directed mutagenesis reaction was performed in a final volume of 50  $\mu$ l containing 1 ng/ $\mu$ l template DNA, 2.5 ng/ $\mu$ l each primer, 200  $\mu$ M each deoxynucleoside triphosphate, 2.5 U of PfuTurbo DNA polymerase (Stratagene, La Jolla, CA, USA), 10 mM KCl, 10 mM  $(\text{NH}_4)_2\text{SO}_4$ , 20 mM Tris-HCl (pH 8.8), 2 mM  $\text{MgSO}_4$ , 0.1% Triton X-100, and 100 ng/ $\mu$ l bovine serum albumin (BSA). Reactions were carried out in a PTC-200 DNA thermal cycler (MJ Research, Cambridge, MA, USA) with an initial denaturation step (95  $^\circ\text{C}$ , 30 s) followed by 20 cycles of denaturation (95  $^\circ\text{C}$ , 30 s), annealing (55  $^\circ\text{C}$ , 1 min), and extension (68  $^\circ\text{C}$ , 7 min). *DnpI* (20 U, New England Biolabs, Ipswich, MA, USA) subsequently was added to each reaction, and digests were allowed to incubate at 37  $^\circ\text{C}$  for 1 h.

### Protein expression and purification

$(\text{His})_6\text{MazE/MazF}$  and  $\text{MazE/MazF}(\text{His})_6$  were expressed using the same procedure. A 20-ml overnight culture of *E. coli* BL21(DE3) transformed with the appropriate expression vector (either pKm6EF or pKmEF6) was used to inoculate 2 L of LB media containing kanamycin (50  $\mu\text{g}/\text{ml}$ ). The bacterial culture was grown at 37  $^\circ\text{C}$  to  $\text{OD}_{600} = 0.4$ , and protein expression was then induced by the addition of isopropyl  $\beta$ -D-1-thiogalactopyranoside (IPTG, Research Products International, Mount Prospect, IL, USA) to a final concentration of 1.0 mM. The culture was allowed to grow for an additional 4 h. Cells were then harvested by centrifugation and stored in pellets (corresponding to 1 L of culture) at  $-20$   $^\circ\text{C}$ .

Protocols for protein purification were modified from protocols reported by Zhang and coworkers [24]. To purify  $\text{MazF}(\text{His})_6$ , a  $\text{MazE/MazF}(\text{His})_6$  expression pellet was thawed at room temperature and resuspended in 10 ml of cold binding buffer (50 mM Tris-Cl, 300 mM NaCl, and 10 mM imidazole at pH 8.0). Cells subsequently were lysed by sonication, and lysate was centrifuged (35,000g for 30 min). Subsequent steps of purification of MazEF from the supernatant were performed at 4  $^\circ\text{C}$ . The protein complex was trapped on nickel-nitrilotriacetate (Ni-NTA) resin by mixing 2 ml of Qiagen NTA resin with the supernatant by inversion for 1 h. Resin was then washed with 10 ml of binding buffer containing 8 M urea to disrupt the MazE/MazF interaction and remove MazE. This was followed by seven washes of 10 ml urea/binding buffer, with the concentration of urea decreasing by 1 M each wash to slowly refold the protein on the column. The resin was then washed with 10 ml of binding buffer and 10 ml of wash buffer (50 mM Tris-Cl, 300 mM NaCl, and 20 mM imidazole at pH 8.0).  $\text{MazF}(\text{His})_6$  was eluted with 5 ml of elution buffer (50 mM Tris-Cl, 300 mM NaCl, and 250 mM imidazole at pH 8.0), and the elution was collected in five 1-ml fractions.  $(\text{His})_6\text{MazE}$  was purified in

a manner analogous to that described above for  $(\text{His})_6\text{MazE/MazF}$  expression pellets.

Protein concentration was determined by Bradford assay. To enhance the accuracy of these concentration measurements, calibration curves were constructed for each protein by performing the Bradford assay on resolubilized lyophilized protein of known mass. As these calibration curves were used in future experiments to relate absorbance values from the Bradford assay to protein concentration, the Bradford assay was performed in exactly the same manner every time. To perform this assay, 60  $\mu$ l of water was added to 20  $\mu$ l of protein solution in a well of a 96-well plate. Then 20  $\mu$ l of Bradford assay dye (Bio-Rad Laboratories, Hercules, CA, USA) was added to the well and mixed by pipetting. The absorbance of the well at 595 nm was read exactly 10 min after the addition of Bradford assay dye to the well. The calibration curves for  $\text{MazE/MazF}(\text{His})_6$ ,  $(\text{His})_6\text{MazE/MazF}$ ,  $\text{MazF}(\text{His})_6$ , and  $(\text{His})_6\text{MazE}$  are shown in [Supplementary Fig. 1](#). Elution fractions for both proteins were stored on ice for no more than 2 h before they were used in experiments as a decrease in  $\text{MazF}(\text{His})_6$  activity was observed with longer storage times.

### HPLC analysis of oligonucleotide cleavage products

A 250- $\mu$ l solution of 11.5  $\mu\text{M}$   $\text{MazF}(\text{His})_6$  (or 3  $\mu\text{M}$   $\text{MazE/MazF}(\text{His})_6$ ) and 24  $\mu\text{M}$  chimeric oligonucleotide of the sequence 5'-AAGTCrGACATCAG-3' in elution buffer was allowed to incubate for 5 h at room temperature. The reaction mixture subsequently was flash frozen in liquid nitrogen. A 100- $\mu$ l portion of each thawed reaction mixture was analyzed by high-performance liquid chromatography (HPLC) using a BioCad SPRINT liquid chromatograph (260-nm detector). An Xterra MS C18 column (10  $\times$  50 mm, 2.5  $\mu\text{m}$ , Waters, Milford, MA, USA) was used to separate intact oligonucleotide from cleavage fragments with a linear gradient from 0.1 M triethylammonium acetate (TEAA) (pH 7.0) to 0.085 M TEAA/15% acetonitrile (pH 7.0) over 20 min. Fractions with  $A_{260}$  values greater than 0.01 were collected and lyophilized. Lyophilized oligonucleotide was resuspended in 100  $\mu$ l of RNase-free water and analyzed by MALDI mass spectrometry.

### Fluorescence plate reader settings

Fluorescence was measured on a Criterion Analyst AD (Molecular Devices, Sunnyvale, CA, USA) using a  $485 \pm 15$ -nm excitation filter, a  $530 \pm 15$ -nm emission filter, and a 505-nm cutoff dichroic mirror. The fluorophore was excited with a 1000-W continuous lamp with 10 reads per well.

### Oligonucleotide cleavage assay

Wells of a black 384-well plate were filled with 5  $\mu$ l of the 6-FAM and BHQ1 dually labeled fluorescent oligonucleotide in TE buffer and 10  $\mu$ l of cold elution buffer.

Fluorescence of the filled wells was measured every 20 s for 20 min, at which point 15  $\mu\text{l}$  of either cold elution buffer or MazF was added. Fluorescence subsequently was measured every 20 s for 33.3 min.

#### *Construction of calibration plot*

Solutions containing a 1:1 (mol/mol) mixture of the labeled 5' and 3' cleavage fragments at concentrations of 0.3, 0.6, 1.5, 3.0, 6.0, and 9.0  $\mu\text{M}$  were prepared by dilution with TE buffer. Wells of a black 384-well plate were filled with 5  $\mu\text{l}$  of each solution and 10  $\mu\text{l}$  of cold elution buffer. Fluorescence of the filled wells was measured as described above. A 15- $\mu\text{l}$  portion of cold elution buffer was added to each well after a 20-min read. Fluorescence values at the 20-min time point (20 min after the addition of the second elution buffer) were used to construct a calibration plot of relative fluorescence units (RFU) against oligonucleotide fragment concentration. This experiment was repeated, and a calibration plot was constructed for each plate read.

#### *Kinetic analysis*

Slopes derived from the MazF processing of the labeled substrate were compared with controls in which no enzyme was added. Data obtained for these controls (in which just elution buffer was added) were subtracted from data obtained for the addition of MazF, and the difference was converted from RFU to picomoles oligonucleotide cleaved using the slope obtained from the calibration plot. Microsoft Excel was used to perform linear regression analysis on these data to obtain initial velocities for reactions involving MazF and a range of fluorescent oligonucleotides (0.05–50  $\mu\text{M}$ ). The initial velocities were plotted against substrate concentration and, using KaleidaGraph software (Synergy Software, Reading, PA, USA), the Michaelis–Menten equation was fit to the data for oligonucleotide concentrations less than 0.3  $\mu\text{M}$  and greater than 20  $\mu\text{M}$ .

#### *MazE inhibition studies*

Experiments were performed as described for the oligonucleotide cleavage assay for 20  $\mu\text{M}$  fluorescent oligonucleotide substrate; however, in addition to preparing a reaction by adding MazF(His)<sub>6</sub> alone to the elution buffer/oligonucleotide solution, another reaction was prepared by adding a mixture of separately purified (His)<sub>6</sub>MazE and MazF(His)<sub>6</sub> to final concentrations of 1.5 and 3.0  $\mu\text{M}$ , respectively. The MazE/MazF mixture was allowed to incubate on ice for 10 min before the addition to the well. Data obtained were background subtracted as described above.

#### *Ribonuclease inhibitor protein inhibition studies*

Experiments were performed as described for MazE inhibition studies; however, a 2:1 (v/v) mixture of

MazF(His)<sub>6</sub> and Protector RNase Inhibitor (Roche, Nutley, NJ, USA) was added to the oligonucleotide/elution buffer solution to a final concentration of 3  $\mu\text{M}$  and 6.7 U/ $\mu\text{l}$ , respectively. The reaction involving MazF(His)<sub>6</sub> alone was prepared in such a way that a 2:1 (v/v) mixture of MazF(His)<sub>6</sub> and ribonuclease inhibitor storage buffer (50 mM Hepes [pH 7.6], 20 mM potassium chloride, 8 mM dithiothreitol [DTT], and 50% glycerol) was added to account for the effect of DTT and glycerol on reaction velocity.

#### *Adenosine 3',5'-diphosphate inhibition studies*

Experiments were performed as described for MazE inhibition studies. A solution of MazF(His)<sub>6</sub> and adenosine 3',5'-diphosphate (pAp) were added to the oligonucleotide/elution buffer solution to a final concentration of 3  $\mu\text{M}$  and 1 mM, respectively.

#### *High-throughput screen simulation*

A 25- $\mu\text{l}$  solution of 0.9  $\mu\text{M}$  MazE/MazF(His)<sub>6</sub> was delivered to all wells of a black 384-well plate, excluding wells in column 24 and wells M3, J7, G13, and C18. Column 24 was reserved for control reactions (25  $\mu\text{l}$  of elution buffer in A, B, and C; 25  $\mu\text{l}$  of 0.9  $\mu\text{M}$  MazE/MazF(His)<sub>6</sub> in wells D, E, and F; 25  $\mu\text{l}$  of 3.6  $\mu\text{M}$  (His)<sub>6</sub> in wells G, H, and I), and 25  $\mu\text{l}$  of 3.6  $\mu\text{M}$  MazF(His)<sub>6</sub> was pipetted into each of the four remaining wells (M3, J7, G13, and C18). Compounds from an in-house compound collection [26] were delivered to the first 23 columns of the plate via a pin transfer device, and 5  $\mu\text{l}$  of fluorescent oligonucleotide substrate was added to each well to a final concentration of 12.5 nM. Immediately after the addition of substrate ( $t = 0$ ), the fluorescence of each well was measured (excitation = 485 nm, emission = 530 nm). The plate was then allowed to incubate in the dark at room temperature for 2.5 h. The fluorescence of the wells was then measured again, and the fluorescence values for the  $t = 0$  read were subtracted from those obtained after 2.5 h.

## **Results**

#### *Substrate design*

Fluorogenic substrates have been used to analyze ribonuclease kinetics, substrate specificity [27], and inhibition [28–30]. These substrates often are chimeric, as they are composed of a single RNA base flanked by short (1–4 bases) sequences of DNA bases, and they are labeled on one end with a fluorophore and on the other end with a quencher. In an intact oligonucleotide, the fluorophore is in close proximity to the quencher and a low amount of fluorescence is observed. However, on cleavage of the oligonucleotide, the distance between the fluorophore and the quencher increases, resulting in an increase in observed fluorescence.

Short (7–15 bases) chimeric oligonucleotides have been designed to report on MazF activity, and cleavage of the  $^{32}\text{P}$ -labeled versions of these oligonucleotides by MazF has been demonstrated [23]. We used one such oligonucleotide of the sequence 5'-AAGTCrGACATCAG-3' to design a fluorogenic MazF substrate by appending 6-FAM to the 5' end and BHQ1 to the 3' end (Fig. 1). Cleavage of this oligonucleotide by MazF is indicated by an increase in fluorescent emission of 6-FAM at 530 nm and was assessed as described in the sections below.

#### Construction of a calibration curve

A calibration curve relating fluorescence emission at 530 nm to the extent of oligonucleotide substrate cleavage is shown in Fig. 2. Oligonucleotides of identical sequence and labeling to the fluorescent oligonucleotide substrate cleavage products (5'-6-FAM-AAGTCG-3' and 5'-ACATCAG-BHQ1-3') were purchased. For ease of synthesis, the RNA base of the 5' cleavage fragment was replaced with the corresponding DNA base; however, this replacement is not expected to change the fluorescent properties of the cleavage fragment. The two oligonucleotide fragments were mixed in 1:1 molar ratios for various oligonucleotide concentrations to mimic cleavage reactions at various stages of completion, and the fluorescence of the solutions was

quantified by excitation at 485 nm and emission at 530 nm. The calibration curve was linear up to concentrations of 60 pmol (2  $\mu\text{M}$ ) cleaved oligonucleotide and was constructed in parallel to each kinetic experiment.

#### Kinetics of MazF-mediated cleavage of fluorescently labeled chimeric substrate

The sensitivity of the fluorogenic substrate allowed us to study the reaction kinetics of oligonucleotide cleavage by MazF. Solutions of oligonucleotide (at final concentrations ranging from 0.1 to 50  $\mu\text{M}$ ) were prepared and distributed in the wells of a 384-well plate. MazF(His)<sub>6</sub> was added to a final concentration of 3  $\mu\text{M}$ , and the reaction progress was monitored by observing the fluorescence emission at 530 nm after excitation at 485 nm. On the addition of elution buffer to oligonucleotide substrate, an initial increase in fluorescence was observed (see Supplementary Fig. 2A). This increase is not due to oligonucleotide cleavage given that the same effect was observed on the addition of elution buffer to 6-FAM alone (see Supplementary Fig. 2B). This increase leveled off after 15 min; therefore, each data set was analyzed after this 15-min time period elapsed, as shown in Fig. 3A. Data for the addition of elution buffer alone were then subtracted from data for the addition of MazF to obtain reaction progress curves from

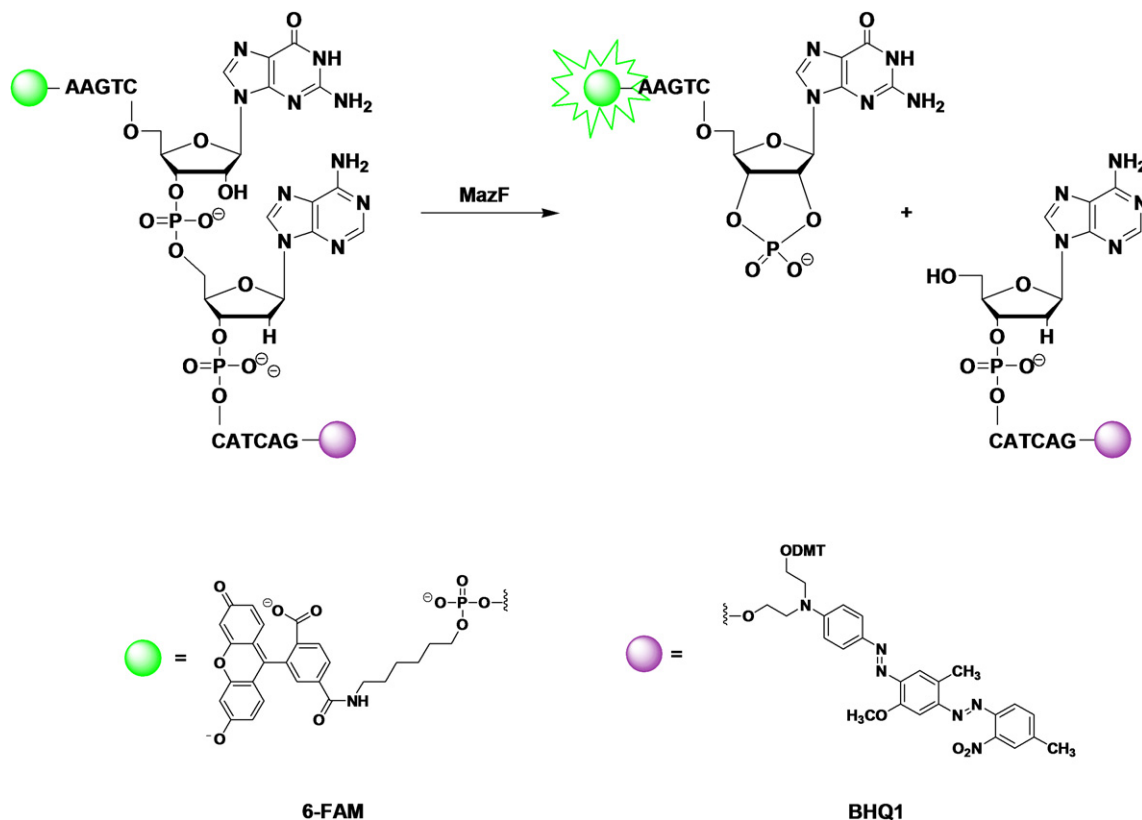


Fig. 1. Substrate design. A chimeric DNA/RNA oligonucleotide (5'-AAGTCrGACATCAG-3') previously shown to be cleaved by MazF was labeled with 6-FAM on the 5' end and with BHQ1 on the 3' end. When the oligonucleotide is intact, BHQ1 quenches the fluorescence of 6-FAM; however, cleavage of the oligonucleotide at the RNA base by MazF releases 6-FAM from BHQ1, thereby increasing the fluorescence of 6-FAM.

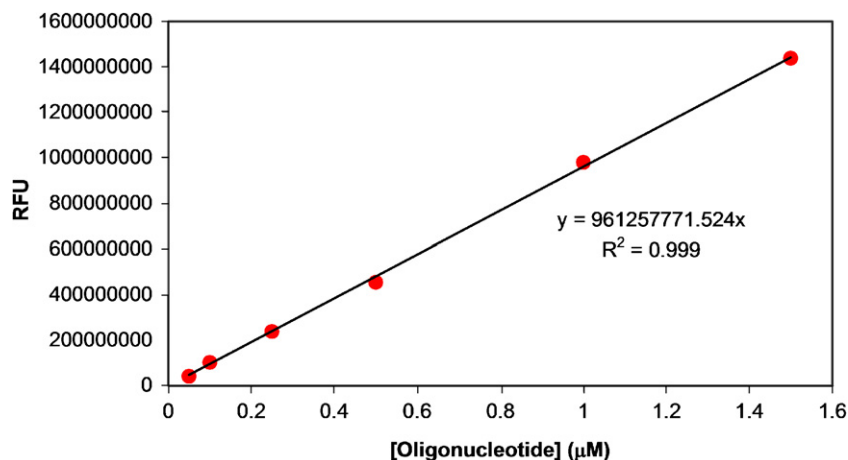


Fig. 2. Construction of a calibration curve. Labeled oligonucleotides corresponding to products formed by cleavage of the fluorescently labeled oligonucleotide substrate by MazF were mixed at 1:1 molar ratios for various concentrations. Fluorescence values for these 1:1 mixtures in elution buffer were measured on excitation at 485 nm and emission at 530 nm, allowing the construction of a calibration curve that relates fluorescence to the amount of oligonucleotide cleaved. Calibration curves were linear up to 60 pmol (2  $\mu\text{M}$ ) of each cleavage fragment. A calibration curve was constructed in parallel with every experiment.

which reaction velocities could be calculated. Reaction velocity increases with increasing substrate concentration, as shown in Fig. 3B.

Reaction velocities were measured in this manner for three separate batches of purified MazF(His)<sub>6</sub> (see Supplementary Fig. 3 for raw data from each of these three trials), and the average velocities were plotted against oligonucleotide substrate concentration (Fig. 3C). The shape of the plotted data indicates that the cleavage reaction follows Michaelis–Menten kinetics; however, because 3  $\mu\text{M}$  MazF(His)<sub>6</sub> was used in each reaction, there are several reactions for which the oligonucleotide substrate concentration is less than or equal to the enzyme concentration. Thus, standard kinetic analysis of enzymatic reactions dictate that the Michaelis–Menten equation could not be fit to the entire data set [31]. An equation similar to the Michaelis–Menten equation,

$$v = \frac{V_{\max}[\text{Substrate}]}{K_s + [\text{Substrate}]},$$

where  $K_s$  is the dissociation constant for the enzyme/substrate complex, can be fit to data where the enzyme concentration is at least 10-fold greater than the substrate concentration [31]; therefore, this equation can be used to describe the MazF(His)<sub>6</sub> reactions with oligonucleotide substrate of 0.3  $\mu\text{M}$  or less. It has been shown that for enzymatic reactions with a low turnover number ( $k_{\text{cat}}$ ),  $K_M$  is approximately equal to  $K_s$  [32]; in this case, the above equation is equivalent to the Michaelis–Menten equation. Analysis of the plotted data in Fig. 3C indicated that the  $k_{\text{cat}}$  for oligonucleotide cleavage by MazF was low given that a large concentration (3  $\mu\text{M}$ ) of MazF was required to achieve moderate values for  $V_{\max}$ . Thus, the Michaelis–Menten equation was fit to data for oligonucleotide concentrations of 0.3  $\mu\text{M}$  or lower and 20  $\mu\text{M}$  or high-

er. From the curve fit,  $V_{\max} = 0.37 \pm 0.02$  pmol/min and  $K_M = 6.9 \pm 1.9$   $\mu\text{M}$ .

#### *Analysis of MazF cleavage of chimeric substrate by liquid chromatography and mass spectrometry*

To verify that the fluorescence increase observed on incubation of MazF with oligonucleotide substrate is indeed due to cleavage by MazF, reaction products were analyzed by HPLC. A 24- $\mu\text{M}$  solution of unlabeled oligonucleotide (5'-AAGTCrGACATCAG-3') was incubated for 5 h with either 11.5  $\mu\text{M}$  MazF(His)<sub>6</sub> or 5.75  $\mu\text{M}$  MazE plus 11.5  $\mu\text{M}$  MazF(His)<sub>6</sub> as a 2:4 complex. As shown in Fig. 4, the HPLC trace of the oligonucleotide reaction with MazE/MazF(His)<sub>6</sub> contained a single peak at a retention time of 14.3 min, whereas the trace for the reaction with MazF(His)<sub>6</sub> contained two peaks at lower retention times. Analysis of the elution fractions corresponding to each peak by MALDI mass spectrometry revealed that the peak at the longer retention time corresponded to  $m/z$  3983.82, the mass of intact unlabeled oligonucleotide (see Supplementary Fig. 4A for mass spectrum). The peaks produced in the presence of MazF(His)<sub>6</sub> correspond to  $m/z$  1890.6 and 2088.7, the masses of the oligonucleotide fragments produced by MazF cleavage of the unlabeled oligonucleotide (see Supplementary Fig. 4B and C for mass spectra). The unlabeled oligonucleotide substrate is cleaved at the RNA base by MazF(His)<sub>6</sub> in the absence, but not in the presence, of MazE (see Supplementary Fig. 4D for mass spectrum). Thus, we conclude that MazF cleaves labeled oligonucleotide substrate in a similar manner and that the increase in fluorescence observed in the presence of MazF is indeed a direct result of this cleavage event.

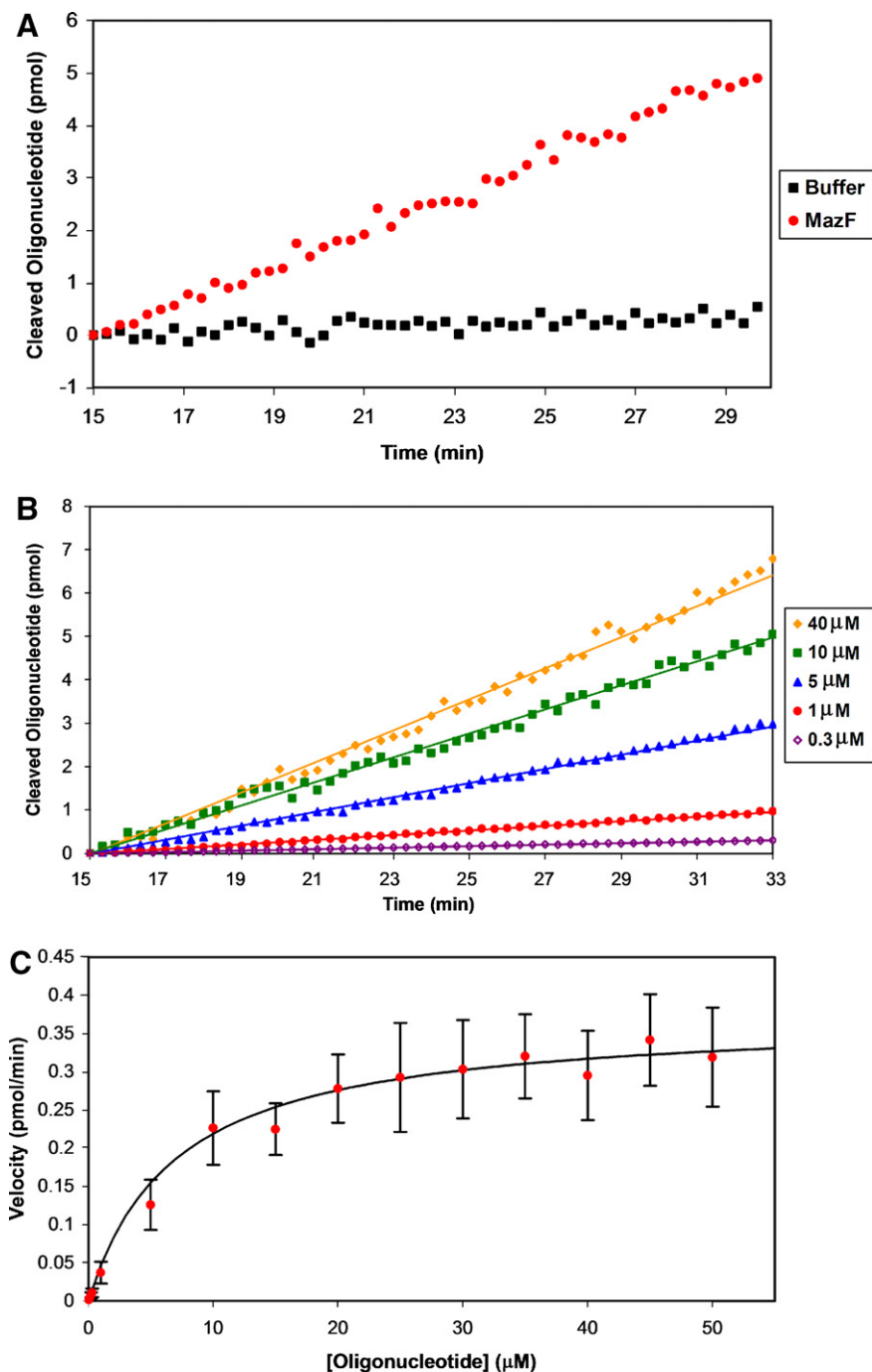


Fig. 3. Determination of kinetic parameters for substrate cleavage by MazF. MazF (final concentration of 3  $\mu\text{M}$ ) was added to various concentrations of oligonucleotide substrate, and fluorescence was monitored on excitation at 485 nm and emission at 530 nm. (A) Data analysis began 15 min after the addition of MazF or elution buffer. The change in 6-FAM emission with reaction progress is shown for the addition of MazF (red circles) and elution buffer (black squares) to a solution of 20  $\mu\text{M}$  of the fluorescently labeled chimeric substrate. Data for the addition of elution buffer were then subtracted from data for the addition of MazF, and the resulting data were used to construct the plots shown in panel B. (B) Linear regression analysis was performed on the background-subtracted data set for each oligonucleotide substrate concentration. Shown are data sets for substrate at 40  $\mu\text{M}$  (filled yellow diamonds), 10  $\mu\text{M}$  (filled green squares), 5  $\mu\text{M}$  (filled blue triangles), 1  $\mu\text{M}$  (filled red circles), and 0.3  $\mu\text{M}$  (empty purple diamonds). (C) The slopes from the data sets shown in panel B were plotted against oligonucleotide substrate concentration. Reaction velocities were determined for three separate batches of purified MazF, and average velocities are plotted. Error bars represent the standard deviation from the mean. The Michaelis–Menten equation was fit to the data for substrate concentrations  $\leq 0.3 \mu\text{M}$  and  $\geq 20 \mu\text{M}$ . From the curve fit,  $V_{\text{max}} = 0.37 \pm 0.02 \text{ pmol/min}$  and  $K_{\text{M}} = 6.9 \pm 1.9 \mu\text{M}$ . (For interpretation of the references to color in this figure legend, the reader is referred to the Web version of this article.)

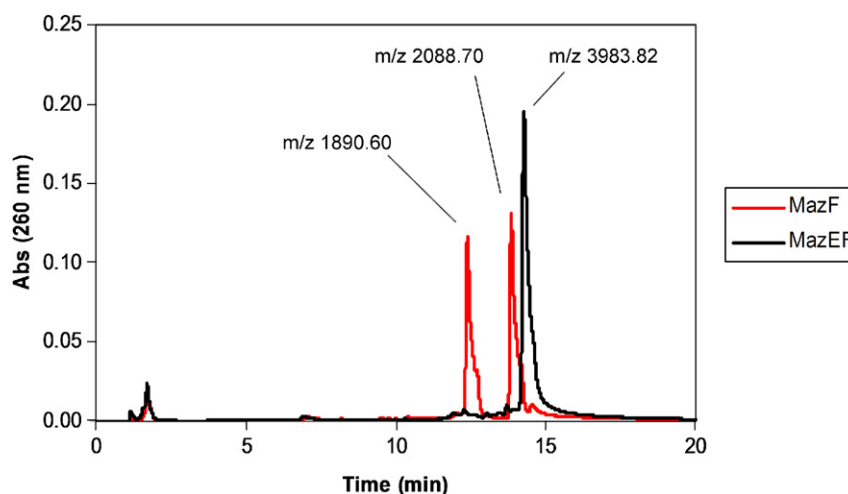


Fig. 4. Verification of substrate cleavage by HPLC. Products from a 5-h incubation of 24  $\mu\text{M}$  unlabeled chimeric oligonucleotide (5'-AAGTCrGACATCAG-3') with 11.5  $\mu\text{M}$  MazF(His)<sub>6</sub> in the presence (black) and absence (red) of 5.75  $\mu\text{M}$  MazE were observed by HPLC analysis. Peak fractions were analyzed by MALDI mass spectrometry. The peak at longest retention time corresponds to intact oligonucleotide (calculated molecular weight [MW] = 3983.6). The peaks at shorter retention times correspond to 5' and 3' fragments generated from MazF cleavage (calculated MWs = 1894.2 and 2088.4, respectively). (For interpretation of the references to color in this figure legend, the reader is referred to the Web version of this article.)

#### Use of fluorescent substrate to assess inhibitors of MazF

The assay was also used to investigate the effect of various ribonuclease inhibitors on MazF activity. The only reported inhibitor of MazF to date is MazE; thus, the effect of MazE on MazF cleavage of the fluorescent oligonucleotide substrate was investigated. As expected, the addition of 1.5  $\mu\text{M}$  MazE abolishes the activity of 3.0  $\mu\text{M}$  MazF against 20  $\mu\text{M}$  oligonucleotide substrate (Fig. 5A). Thus, the fluorescent oligonucleotide substrate can be used to detect MazF inhibition.

The products of oligonucleotide cleavage by MazF, most notably a 2',3'-cyclic phosphodiester on the 3' end of the 5' fragment (Fig. 1), have been shown to be similar to those observed on oligonucleotide cleavage by RNase A. Therefore, it has been suggested that MazF and RNase A cleave RNA via a similar mechanism [23]. If this were true, one might expect that certain RNase A inhibitors would also inhibit MazF. To test this, we incubated MazF with fluorescent oligonucleotide substrate in the presence of two RNase A inhibitors: ribonuclease inhibitor protein (RI, 200 U) and adenosine 3',5'-diphosphate (pAp, 1 mM) [33,34]. Neither RNase A inhibitor resulted in a decrease in velocity of the MazF/oligonucleotide substrate reaction (Fig. 5B and C); thus, neither inhibitor inhibits MazF to any appreciable extent at the concentrations evaluated.

#### Use of fluorescent substrate as a reporter of MazEF disruption in a high-throughput screen

The expression of MazF without MazE has been shown to reduce cell viability [35]; thus, it has been speculated that small molecule disruptors of the MazE/MazF complex could function as novel antibiotics [5]. The identification of such a small molecule disruptor could potentially be dis-

covered via high-throughput screening of a large library of compounds. The fluorescent oligonucleotide substrate reported in this article could be an integral component of such a screen given that the disruption of the MazE/MazF complex would release active MazF to cleave the substrate, resulting in an increase in fluorescence. To assess the utility of our fluorescent oligonucleotide substrate in this capacity, all but four wells of the first 23 columns of a black 384-well plate were filled with 25  $\mu\text{l}$  of a MazE/MazF(His)<sub>6</sub> solution. MazE and MazF form a 2:4 complex; thus, the final concentrations in these solutions are 1.5  $\mu\text{M}$  MazE and 3.0  $\mu\text{M}$  MazF. The remaining four wells were filled with 25  $\mu\text{l}$  of MazF(His)<sub>6</sub> to a final concentration of 3.0  $\mu\text{M}$ . Compounds from an in-house collection [26] were delivered to the plate via a pin transfer device, and 5  $\mu\text{l}$  of substrate was then pipetted into all wells to a final concentration of 12.5 nM. Column 24 of the plate was reserved for controls. Three wells of this column were filled with 25  $\mu\text{l}$  of elution buffer, three wells were filled with 25  $\mu\text{l}$  of the MazE/MazF(His)<sub>6</sub> solution, and another three wells were filled with 25  $\mu\text{l}$  of the MazF(His)<sub>6</sub> solution. A 5- $\mu\text{l}$  solution of the substrate was added to all wells of the 384-well plate, and after 2.5 h incubation at room temperature the fluorescence (excitation = 485 nm, emission = 530 nm) of all wells was analyzed. Wells containing MazF were easily distinguishable from those containing MazE/MazF(His)<sub>6</sub>, indicating that a small molecule disruptor of the MazE/MazF complex would indeed be detectable using this substrate (Fig. 6). It should be noted that very low concentrations (12.5 nM) of the substrate can be used in these experiments, making it practical on the large scale required for screening thousands of compounds.

This article has described a simple and convenient method for the detailed assessment of MazF activity, and we used this assay to determine  $K_M$  and  $V_{\text{max}}$  values for

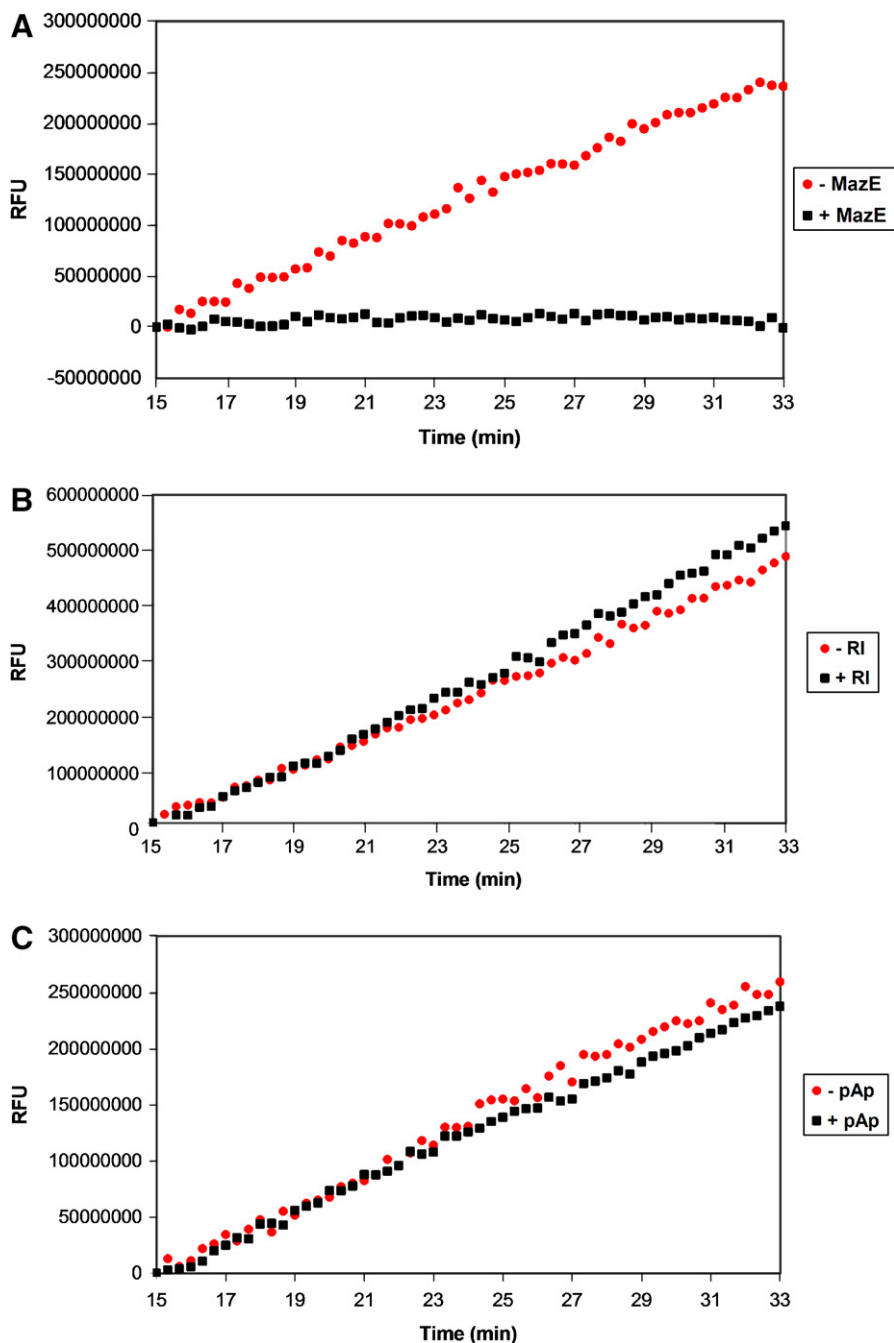


Fig. 5. Assessment of MazF activity in the presence of ribonuclease inhibitors. Various ribonuclease inhibitors were added to MazF and elution buffer prior to their addition to oligonucleotide substrate. The effects of inhibitors on reaction velocity were monitored by fluorescence quantification by excitation at 485 nm and emission at 530 nm. (A) A mixture of MazF and MazE was added to oligonucleotide substrate to final concentrations of 3.0  $\mu\text{M}$  MazF and 1.5  $\mu\text{M}$  MazE. Inhibition of MazF by MazE is indicated by the static fluorescence observed after the addition of MazF/MazE (black squares) in comparison with the increase in fluorescence observed after the addition of MazF alone (red circles). (B) A MazF/ribonuclease inhibitor (RI) solution was added to oligonucleotide substrate to final concentrations of 3  $\mu\text{M}$  MazF and 200 U RI. No inhibition of MazF by RI is observed given that the fluorescence change of the oligonucleotide/MazF solution is the same in the presence and absence of RI. (C) An experiment similar to that described in panel B was repeated for the RNase A inhibitor pAp. Again, no inhibition of MazF by pAp is observed given that the fluorescence change of the reaction solution is the same in the presence and absence of 1 mM pAp. (For interpretation of the references to color in this figure legend, the reader is referred to the Web version of this article.)

MazF. The assay can be performed easily in 384-well plates and can be run with commercially available materials. Interestingly, two common ribonuclease inhibitors, RI and pAp, do not inhibit the MazF-catalyzed reaction.

Because MazEF appears to be part of a larger family of TA systems [36], this assay should be useful in studying the entire family of MazEF-like proteins. Through use of this assay, unresolved questions about the substrate

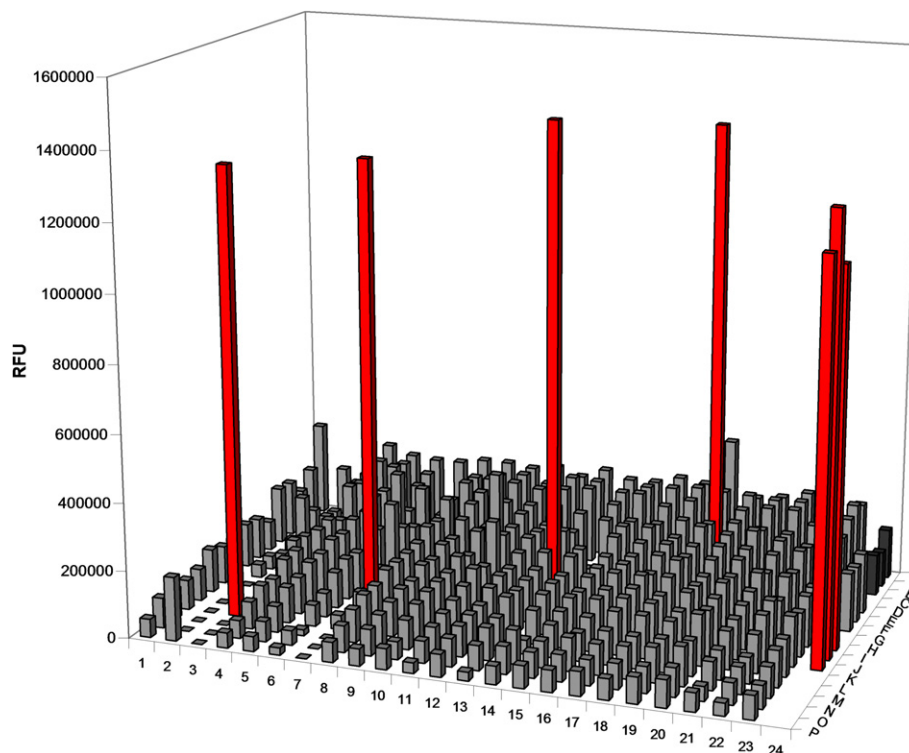


Fig. 6. High-throughput screen simulation. A 12.5-nM solution of the fluorescently labeled oligonucleotide substrate was incubated in wells of a 384-well plate filled with either MazE/MazF(His)<sub>6</sub> (1.5:3.0 μM) or MazF(His)<sub>6</sub> (3 μM). Control wells were prepared in column 24, where oligonucleotide was incubated in the absence of compound with elution buffer (dark gray), MazE/MazF(His)<sub>6</sub> (1.5:3.0 μM, light gray), and MazF(His)<sub>6</sub> (red). After a 2.5-h incubation, wells containing MazF(His)<sub>6</sub> (M3, J7, G13, and C18) are easily distinguished from those containing MazE/MazF(His)<sub>6</sub>. These results demonstrate that the fluorescent oligonucleotide substrate could be used to detect MazEF complex disruptors in a high-throughput screen. (For interpretation of the references to color in this figure legend, the reader is referred to the Web version of this article.)

specificity of MazF can now be answered in a facile manner, and the novel substrate reported here should also facilitate high-throughput screens aimed at the identification of MazF inhibitors or MazE/MazF disruptors.

### Acknowledgments

This work was supported by the National Institutes of Health (R01-GM68385) and the Office of Naval Research (N00014-02-1-0390). N.R.W. was supported through the Department of Homeland Security (DHS) Scholarship and Fellowship Program.

### Appendix A. Supplementary data

Supplementary data associated with this article can be found, in the online version, at [doi:10.1016/j.ab.2007.07.017](https://doi.org/10.1016/j.ab.2007.07.017).

### References

- [1] U. Zielenkiewicz, P. Ceglowski, Mechanisms of plasmid stable maintenance with special focus on plasmid addiction systems, *Acta Biochim. Pol.* 4 (2001) 1003–1023.
- [2] K. Gerdes, S.K. Christensen, A. Lobner-Olesen, Prokaryotic toxin–antitoxin stress response loci, *Nat. Rev. Microbiol.* 5 (2005) 371–382.
- [3] F. Hayes, Toxins–antitoxins: plasmid maintenance, programmed cell death, and cell cycle arrest, *Science* 303 (2003) 1496–1499.
- [4] D.P. Pandey, K. Gerdes, Toxin–antitoxin loci are highly abundant in free-living but lost from host-associated prokaryotes, *Nucleic Acids Res.* 33 (2005) 966–976.
- [5] E.M. Moritz, P.J. Hergenrother, Toxin–antitoxin systems are ubiquitous and plasmid-encoded in vancomycin-resistant enterococci, *Proc. Natl. Acad. Sci. USA* 104 (2007) 311–316.
- [6] K. Gerdes, P.B. Rasmussen, S. Molin, Unique type of plasmid maintenance function: Postsegregational killing of plasmid-free cells, *Proc. Natl. Acad. Sci. USA* 103 (1986) 3116–3120.
- [7] M.B. Yarmolinsky, Programmed cell death in bacterial populations, *Science* 267 (1995) 836–837.
- [8] R.B. Jensen, K. Gerdes, Programmed cell death in bacteria: proteic plasmid stabilization systems, *Mol. Microbiol.* 2 (1995) 205–210.
- [9] R. Hazan, B. Sat, H. Engelberg-Kulka, *Escherichia coli* mazEF-mediated cell death is triggered by various stressful conditions, *J. Bacteriol.* 186 (2004) 3663–3669.
- [10] B. Sat, M. Reches, H. Engelberg-Kulka, The *Escherichia coli* mazEF suicide module mediates thymineless death, *J. Bacteriol.* 185 (2003) 1803–1807.
- [11] B. Sat, R. Hazan, T. Fisher, H. Khaner, G. Glaser, H. Engelberg-Kulka, Programmed cell death in *Escherichia coli*: some antibiotics can trigger mazEF lethality, *J. Bacteriol.* 183 (2001) 2041–2045.
- [12] S.K. Christensen, M. Mikkelsen, K. Pedersen, K. Gerdes, RelE, a global inhibitor of translation, is activated during nutritional stress, *Proc. Natl. Acad. Sci. USA* 98 (2001) 14328–14333.
- [13] S.K. Christensen, K. Pedersen, F.G. Hansen, K. Gerdes, Toxin–antitoxin loci as stress-response-elements: ChpAK/MazF and ChpBK

- cleave translated RNAs and are counteracted by tmRNA, *J. Mol. Biol.* 4 (2003) 809–819.
- [14] M.N. Alekshun, S.B. Levy, Molecular mechanisms of antibacterial multidrug resistance, *Cell* 6 (2007) 1037–1050.
- [15] E.M. Moritz, P.J. Hergenrother, The prevalence of plasmids and other mobile genetic elements in clinically important drug-resistant bacteria, in: C. Amábile-Cuevas (Ed.), *Antimicrobial Resistance in Bacteria*, Horizon Scientific, Norfolk, UK, 2007.
- [16] H. Engelberg-Kulka, B. Sat, M. Reches, S. Amitai, R. Hazan, Bacterial programmed cell death systems as targets for antibiotics, *Trends Microbiol.* 2 (2004) 66–71.
- [17] J.C. DeNap, P.J. Hergenrother, Bacterial death comes full circle: targeting plasmid replication in drug-resistant bacteria, *Org. Biomol. Chem.* 6 (2005) 959–966.
- [18] S. Metzger, I.B. Dror, E. Aizenman, G. Schreiber, M. Toone, J.D. Friesen, M. Cashel, G. Glaser, The nucleotide sequence and characterization of the relA gene of *Escherichia coli*, *J. Biol. Chem.* 30 (1988) 15699–15704.
- [19] Y. Masuda, K. Miyakawa, Y. Nishimura, E. Ohtsubo, chpA and chpB, *Escherichia coli* chromosomal homologs of the pem locus responsible for stable maintenance of plasmid R100, *J. Bacteriol.* 21 (1993) 6850–6856.
- [20] K. Kamada, F. Hanaoka, S.K. Burley, Crystal structure of the MazE/MazF complex: molecular bases of antidote–toxin recognition, *Mol. Cell* 4 (2003) 875–884.
- [21] H. Engelberg-Kulka, R. Hazan, S. Amitai, mazEF: a chromosomal toxin–antitoxin module that triggers programmed cell death in bacteria, *J. Cell Sci.* 118 (2005) 4327–4332.
- [22] H. Engelberg-Kulka, S. Amitai, I. Kolodkin-Gal, R. Hazan, Bacterial programmed cell death and multicellular behavior in bacteria, *PLoS Genet.* 10 (2006) e135.
- [23] Y. Zhang, J. Zhang, H. Hara, I. Kato, M. Inouye, Insights into the mRNA cleavage mechanism by MazF, an mRNA interferase, *J. Biol. Chem.* 5 (2005) 3143–3150.
- [24] Y. Zhang, J. Zhang, K.P. Hoeflich, M. Ikura, G. Qing, M. Inouye, MazF cleaves cellular mRNAs specifically at ACA to block protein synthesis in *Escherichia coli*, *Mol. Cell* 4 (2003) 913–923.
- [25] A.J. Munoz-Gomez, S. Santos-Sierra, A. Berzal-Herranz, M. Lemonnier, R. Diaz-Orejas, Insights into the specificity of RNA cleavage by the *Escherichia coli* MazF toxin, *FEBS Lett.* 2/3 (2004) 316–320.
- [26] P.J. Hergenrother, Obtaining and screening compound collections: a user’s guide and a call to chemists, *Curr. Opin. Chem. Biol.* 3 (2006) 213–218.
- [27] C. Park, B.R. Kelemen, T.A. Klink, R.Y. Sweeney, M.A. Behlke, S.R. Eubanks, R.T. Raines, Fast, facile, hypersensitive assays for ribonucleolytic activity, *Methods Enzymol.* 341 (2001) 81–94.
- [28] L.E. Bretscher, R.L. Abel, R.T. Raines, A ribonuclease A variant with low catalytic activity but high cytotoxicity, *J. Biol. Chem.* 14 (2000) 9893–9896.
- [29] B.R. Kelemen, T.A. Klink, M.A. Behlke, S.R. Eubanks, P.A. Leland, R.T. Raines, Hypersensitive substrate for ribonucleases, *Nucleic Acids Res.* 18 (1999) 3696–3701.
- [30] T.A. Klink, R.T. Raines, Conformational stability is a determinant of ribonuclease A cytotoxicity, *J. Biol. Chem.* 23 (2000) 17463–17467.
- [31] S. Schnell, P.K. Maini, A century of enzyme kinetics: reliability of the  $K_m$  and  $V_{max}$  estimates, *Comments Theor. Biol.* 8 (2003) 169–187.
- [32] I.H. Segel, *Enzyme Kinetics: Behavior and Analysis of Rapid Equilibrium and Steady State Enzyme Systems*, John Wiley, New York, 1975.
- [33] N. Russo, R. Shapiro, B.L. Vallee, 5(-Diphosphoadenosine 3(-phosphate is a potent inhibitor of bovine pancreatic ribonuclease A, *Biochem. Biophys. Res. Commun.* 231 (1997) 671–674.
- [34] G.I. Yakovlev, V.A. Mitkevich, A.A. Makarov, Ribonuclease inhibitors, *Mol. Biol.* 6 (2006) 867–874.
- [35] I. Kolodkin-Gal, H. Engelberg-Kulka, Induction of *Escherichia coli* chromosomal mazEF by stressful conditions causes an irreversible loss of viability, *J. Bacteriol.* 9 (2006) 3420–3423.
- [36] G. Mittenhuber, Occurrence of mazEF-like antitoxin/toxin systems in bacteria, *J. Mol. Microbiol. Biotechnol.* 2 (1999) 295–302.